CSIRO PUBLISHING

Aust. J. Chem. **2013**, *66*, 555–563
http://dx.doi.org/10.1071/CH12564

Full Paper

Cytotoxicity In Vitro, Apoptosis, Cellular Uptake, Cell Cycle Distribution, Mitochondrial Membrane Potential Detection, DNA Binding, and Photocleavage of Ruthenium(II) Complexes

Gan-Jian Lin,[A] *Zheng-Zheng Li,*[A] *Jun-Hua Yao,*[B] *Hong-Liang Huang,*[C,D] *Yang-Yin Xie,*[A] *and Yun-Jun Liu*[A,D]

[A]School of Pharmacy, Guangdong Pharmaceutical University, Guangzhou, 510006, China.
[B]Instrument Analysis and Research Center, Sun Yat-Sen Uiversity, Guangzhou, 510275, China.
[C]School of Life Science and Biopharmaceutical, Guangdong Pharmaceutical University, Guangzhou, 510006, China.
[D]Corresponding authors. Email: hhongliang@163.com; lyjche@163.com

Four new ruthenium(II) complexes $[Ru(bpy)_2(NHPIP)](ClO_4)_2$ (**Ru-1**), $[Ru(phen)_2(NHPIP)](ClO_4)_2$ (**Ru-2**), $[Ru(bpy)_2(AHPIP)](ClO_4)_2$ (**Ru-3**), and $[Ru(phen)_2(AHPIP)](ClO_4)_2$ (**Ru-4**) (bpy = 2,2′-bipyridine; phen = 1,10-phenanthroline; NHPIP = 2-(3-nitro-4-hydroxylphenyl)imidazo[4,5-*f*][1,10]phenanthroline; AHPIP = 2-(3-amino-4-hydroxylphenyl) imidazo[4,5-*f*][1,10]phenanthroline) were synthesized and characterized by elemental analysis, electrospray mass spectrometry, and ^{1}H NMR spectroscopy. The cytotoxicity in vitro of these complexes against BEL-7402, HeLa, MG-63, and MCF-7 cells was evaluated by the MTT (3-(4,5-dimethylthiazol-2-yl)-2,5-diphenyltetrazolium bromide) method. **Ru-4** shows the highest cytotoxic activity towards the selected cell lines among the four complexes. The morphological apoptosis was assayed by an acridine orange/ethidium bromide staining method, and the percentages of necrotic and apoptotic cells were determined by flow cytometry. The cellular uptake and the cell cycle arrest in BEL-7402 cell was investigated. The results showed these complexes inhibit the proliferation of BEL-7402 cells at G0/G1 phase arrest. The detection of mitochondrial membrane potentials using the fluorescence probe JC-1 (5,5′,6,6′-tetrachloro-1,1′,3,3′-tetraethylbenzimidazolcarbocyanine iodide) exhibited that the mitochondrial membrane potentials decrease. Upon irradiation, these complexes can effectively cleave pBR322 DNA.

Manuscript received: 7 November 2012.
Manuscript accepted: 7 January 2013.
Published online: 5 February 2013.

Introduction

Stable, inert, coordinatively saturated, and water-soluble ruthenium complexes are ideally suited and extremely valuable as non-covalent probes of both structural and functional aspects of nucleic acid chemistry.[1–4] A majority of the reported ruthenium complexes contain two bipyridine or phenanthroline units as ancillary ligands. Some of the complexes exhibit unique characteristics, for example, $[Ru(bpy)_2(dppz)]^{2+}$ (bpy = 2,2′-bipyridine; dppz = dipyrido[3,2-*a*:2′,3′-*c*]phenazine) shows no luminescence in aqueous solution at ambient temperature, but luminesces brightly upon binding intercalatively with the dppz ligand between adjacent DNA base pairs, displaying the characteristic of a 'molecular light switch'. The ruthenium(II) complex $[Ru(phen)_2(mdpz)]^{2+}$ (phen = 1,10-phenanthroline, mdpz = 7,7-methylenedioxyphenyldipyrido[3,2-*a*:2,3-*c*]phenazine), as the first true molecular light switch, enhances the stability of the triplex RNA structure.[5] These studies on DNA or RNA as binding targets have stimulated the development of ruthenium complexes as anticancer agents. Schatzschneider et al. reported that $[Ru(bpy)_2(dppz)]^{2+}$ can effectively inhibit the proliferation of HT-29 cells, and $[Ru(bpy)_2(dppn)]^{2+}$ can be uptaken and had a low IC_{50} (half maximal inhibitory concentration) value against MCF-7 cells.[6] The chiral Ru^{II} complex Λ-$[Ru(phen)_2(p\text{-}MOPIP)]^{2+}$ (p-MOPIP = 2-(4-methoxylphenyl)imidazo[4,5-*f*][1,10]phenanthroline) shows a high cytotoxic effect towards HepG-2 cells.[7] $[Ru(bpy)_2(dmdpq)]^{2+}$ (dmdpq = 2,9-dimethyldipyrido[3,2-*f*:2′,3′-*h*]-quinoxaline) is not cytotoxic in the dark, but when irradiated with light (> 450 nm), this complex displays potencies superior to cisplatin against A549 cells.[8] $[Ru(Hdpa)_2(dppz)]^{2+}$ exhibits cytotoxicity ~8 times larger than cisplatin against the human cervical epidermoid carcinoma cell line (ME 180).[9] Complexes $[Ru(phen)_2(DBHIP)]^{2+}$ and $[Ru(phen)_2(DNPIP)]^{2+}$ (DBHIP = 2-(3,5-dibromo-4-hydroxyphenyl)imidazo[4,5-*f*][1,10]phenanthroline, DNPIP = 2-(2,4-dinitrophenyl) imidazo[4,5-*f*][1,10]phenanthroline) can effectively suppress the cell proliferation of BEL-7402 cells.[10,11] Based on our previous studies,[11–13] we found that Ru^{II} polypyridyl complexes containing amino or nitro groups as a substituent in the ligands possess

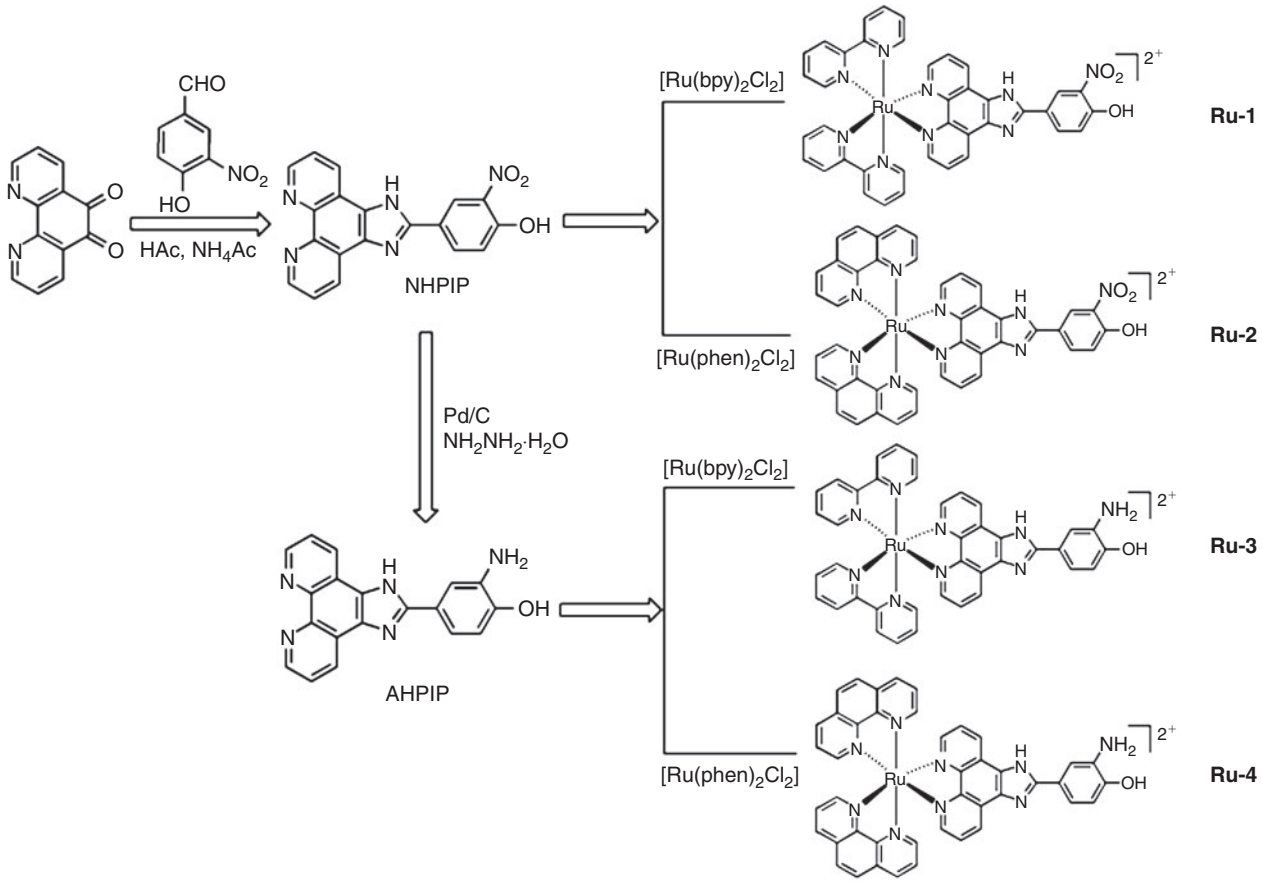

Scheme 1. Synthetic route of ligand and complexes.

significant cytotoxicity in vitro. In order to evaluate further the influence of nitro and amino groups as substituents on the cytotoxic activity in vitro, in this report, two new ligands, NHPIP (2-(3-nitro-4-hydroxylphenyl)imidazo[4,5-*f*][1,10]phenanthroline), containing a nitro group as substituent, and AHPIP (2-(3-amino-4-hydroxylphenyl)imidazo[4,5-*f*][1,10]phenanthroline), obtained by reducing the nitro group into an amino group, and their four Ru^{II} polypyridyl complexes $[Ru(bpy)_2(NHPIP)](ClO_4)_2$ (**Ru-1**), $[Ru(phen)_2(NHPIP)](ClO_4)_2$ (**Ru-2**), $[Ru(bpy)_2(AHPIP)](ClO_4)_2$ (**Ru-3**), and $[Ru(phen)_2(AHPIP)](ClO_4)_2$ (**Ru-4**, Scheme 1) were synthesized and characterized by elemental analysis, electrospray mass spectrometry, and ^1H NMR spectroscopy. Their cytotoxicity in vitro was evaluated by MTT assay (MTT = (3-(4,5-dimethylthiazol-2-yl)-2,5-diphenyltetrazolium bromide)). The morphological apoptosis and the percentage of necrotic and apoptotic cells of BEL-7402 induced by these complexes were also studied by fluorescent microscopy and flow cytometry. The cellular uptake was investigated. The cell cycle distribution induced by the complexes was determined by flow cytometry. The mitochondrial membrane potentials induced by **Ru-1**–**4** were determined under fluorescent microscopy. The DNA binding and photocleavage were also investigated by electronic absorption titration and gel electrophoresis. In addition, the structure–activity relationships are also explored.

Experimental

Materials and Methods

All reagents and solvents were purchased commercially and used without further purification unless specially noted. Ultrapure MilliQ water was used in all experiments. Dimethyl sulfoxide (DMSO) and RPMI 1640 (RPMI = Roswell Park Memorial Institute) were purchased from Sigma. Cell lines of BEL-7402 (human hepatocellular carcinoma cell line), HeLa (human vercix adenocarcinoma cell line), MG-63 (human osteosarcoma cell line), and MCF-7 (human breast cancer cell line) were purchased from American Type Culture Collection. $RuCl_3 \cdot xH_2O$ was purchased from Kunming Institution of Precious Metals. 1,10-Phenanthroline was obtained from Guangzhou Chemical Reagent Factory.

Physical Measurements

Microanalysis (C, H, and N) was carried out with a Perkin–Elmer 240Q elemental analyser. Electrospray ionisation mass spectrometry (ES-MS) was performed on a LCQ system (Finnigan MAT, USA) using methanol as the mobile phase. Fast atom bombardment (FAB) mass spectra were measured on a VG ZAB-HS spectrometer in a 3-nitrobenzyl alcohol matrix. The spray voltage, tube lens offset, capillary voltage, and capillary temperature were set at 4.50 kV, 30.00 V, 23.00 V, and 200°C, respectively, and the quoted *m/z* values are for the major peaks in the isotope distribution. ^1H NMR spectra were recorded on a Varian-500 spectrometer with (D_6)DMSO as solvent and tetramethylsilane as an internal standard at 500 MHz at room temperature.

Synthesis and Characterisation of Ligands and Complexes

Synthesis of Ligand NHPIP

A mixture of 1,10-phenanthroline-5,6-dione (0.315 g, 1.5 mmol),[14] 3-nitro-4-hydroxyphenylaldehyde (0.250 g,

1.5 mmol), ammonium acetate (2.31 g, 30 mmol), and glacial acetic acid (30 cm^3) was refluxed with stirring for 2 h. The cooled solution was diluted with water and neutralized with concentrated aqueous ammonia. The precipitate was collected and purified by column chromatography on silica gel (60–100 mesh) with ethanol as eluent to give the compound as a red powder. Yield: 80 %. Anal. Calc. for $C_{19}H_{11}N_5O_3$: C 63.87, H 3.10, N 19.60. Found: C 63.68, H 3.18, N 19.44 %. *m/z* (FAB) 358 ($[M + H]^+$). δ_H (500 MHz, (D_6)DMSO) 9.05 (dd, 2H, *J* 5.5, 5.0), 9.00 (dd, 2H, *J* 8.1, 8.1), 8.82 (d, 1H, *J* 8.0), 8.02 (s, 1H), 7.80 (dd, 2H, *J* 4.3, 4.4), 6.83 (d, 1H, *J* 8.0), 4.07 (s, 1H).

Synthesis of Ligand NAPIP

NHPIP (0.179 g, 0.5 mmol) was completely dissolved in ethanol (30 cm^3) with stirring for 1 h. Pd/C (0.20 g, 10 % Pd) and $NH_2NH_2{\cdot}H_2O$ (8 cm^3) were then added and the solution refluxed for 6 h. The hot solution was filtered and evaporated to remove the solvent under reduced pressure. The red compound obtained was washed with cool ethanol and dried at 50°C under vacuum. Yield: 72 %. Anal. Calc. for $C_{19}H_{13}N_5O$: C 69.72, H 4.00, N 21.39. Found: C 69.61, H 4.12, N 21.26 %. *m/z* (FAB) 328 ($[M + 1]^+$). δ_H (500 MHz, (D_6)DMSO) 9.00 (dd, 2H, *J* 5.0, 4.5), 8.89 (d, 2H, *J* 8.2), 7.78–7.82 (m, 2H), 7.57 (d, 1H, *J* 7.0), 7.35 (d, 1H, *J* 5.2), 6.82 (d, 1H, *J* 8.5), 4.81 (s, 2H, H_{NH2}), 3.36 (s, 1H, H_{OH}).

*Synthesis of [Ru(bpy)$_2$(NHPIP)](ClO$_4$)$_2$ (**Ru-1**)*

A mixture of *cis*-$[Ru(bpy)_2Cl_2]{\cdot}2H_2O$ (0.260 g, 0.5 mmol)[15] and NHPIP (0.193 g, 0.5 mmol) in ethylene glycol (20 cm^3) was heated at 120°C under argon for 8 h to give a clear red solution. Upon cooling, a red precipitate was obtained by dropwise addition of a saturated aqueous $NaClO_4$ solution. The crude product was purified by column chromatography on neutral alumina with a mixture of MeCN/toluene (3 : 1, v/v) as eluent. The red band was collected. The solvent was removed under reduced pressure and a red powder was obtained. Yield: 71 %. Anal. Calc. for $C_{39}H_{27}N_9Cl_2O_{11}Ru$: C 48.31, H 2.81, N 13.00. Found: C 48.18, H 2.89, N 12.88 %. *m/z* (ES, CH_3CN) 769.4 ($[M - 2ClO_4 - H]^+$), 385.5 ($[M - 2ClO_4]^{2+}$). δ_H (500 MHz, (D_6)DMSO) 8.91 (d, 2H, *J* 8.5), 8.87 (d, 4H, *J* 9.0), 8.78 (s, 1H), 8.21 (t, 2H, *J* 7.0), 8.10 (t, 4H, *J* 7.5), 7.96 (d, 1H, *J* 4.5), 7.84 (d, 4H, *J* 5.0), 7.57–7.61 (m, 4H), 7.35 (t, 2H, *J* 7.0), 6.54 (d, 1H, *J* 8.5), 3.37 (s, 1H).

*Synthesis of [Ru(phen)$_2$(NHPIP)](ClO$_4$)$_2$ (**Ru-2**)*

This complex was synthesized by an identical method as described for **Ru-1**, with *cis*-$[Ru(phen)_2Cl_2]{\cdot}2H_2O$[15] in place of *cis*-$[Ru(bpy)_2Cl_2]{\cdot}2H_2O$. Yield: 70 %. Anal. Calc. for $C_{43}H_{27}N_9Cl_2O_{11}Ru$: C 50.75, H 2.67, N 12.39. Found: C 50.85, H 2.76, N 12.27 %. *m/z* (ES, CH_3CN) 817.6 ($[M - 2ClO_4 - H]^+$), 409.3 ($[M - 2ClO_4]^{2+}$). δ_H (500 MHz, (D_6)DMSO) 9.07 (s, 1H), 8.77 (d, 2H, *J* 8.5), 8.75 (d, 4H, *J* 7.5), 8.39 (s, 4H), 8.14 (d, 2H, *J* 5.0), 8.09 (d, 2H, *J* 5.0), 8.00 (d, 1H, *J* 8.0), 7.94 (d, 2H, *J* 5.0), 7.75–7.79 (m, 6H), 6.61 (d, 1H, *J* 8.0), 3.38 (s, 1H).

*Synthesis of [Ru(bpy)$_2$(AHPIP)](ClO$_4$)$_2$ (**Ru-3**)*

This complex was synthesized by an identical method as described for **Ru-1**, with AHPIP in place of NHPIP. Yield: 71 %. Anal. Calc. for $C_{39}H_{29}N_9Cl_2O_9Ru$: C 49.85, H 3.11, N 13.42. Found: C 49.74, H 3.03, N 13.52 %. *m/z* (ES, CH_3CN) 739.5 ($[M - 2ClO_4 - H]^+$), 370.4 ($[M - 2ClO_4]^{2+}$). δ_H (500 MHz, (D_6)DMSO) 8.86 (dd, 4H, *J* 8.0, 8.0), 8.20 (t, 2H, *J* 6.8), 8.08 (t, 4H, *J* 7.5), 8.02 (d, 2H, *J* 5.5), 7.89–7.94 (m, 4H), 7.86 (d, 2H, *J* 7.6), 7.58 (d, 4H, *J* 7.5), 7.33 (d, 1H, *J* 7.6), 7.02 (d, 1H, *J* 8.0), 6.55 (d, 1H, *J* 8.0), 4.85 (s, 2H), 3.36 (s, 1H).

*Synthesis of [Ru(phen)$_2$(AHPIP)](ClO$_4$)$_2$ (**Ru-4**)*

This complex was synthesized by an identical method as described for **Ru-2**, with AHPIP in place of NHPIP. Yield: 70 %. Anal. Calc. for $C_{43}H_{29}N_9Cl_2O_9Ru$: C 52.29, H 2.96, N 12.76. Found: C 52.40, H 3.07, N 12.63 %. *m/z* (ES, CH_3CN) 787.4 ($[M - 2ClO_4 - H]^+$), 394.5 ($[M - 2ClO_4]^{2+}$). δ_H (500 MHz, (D_6)DMSO) 8.76 (d, 4H, *J* 8.5), 8.38 (s, 4H), 8.11 (d, 2H, *J* 6.0), 8.07 (d, 2H, *J* 6.5), 7.94 (d, 2H, *J* 5.0), 7.74–7.77 (m, 6H), 7.67 (d, 2H, *J* 8.5), 7.64 (d, 1H, *J* 8.0), 7.12 (d, 1H, *J* 6.0), 6.85 (d, 1H, *J* 8.0), 4.83 (s, 2H), 3.35 (s, 1H).

Caution: Perchlorate salts of metal compounds with organic ligands are potentially explosive, and only small amounts of the material should be prepared and handled with great care.

Cytotoxicity Assay In Vitro

MTT assay procedures were used.[16] Cells were placed in 96-well microassay culture plates (8×10^3 cells per well) and grown overnight at 37°C in a 5 % CO_2 incubator. Complexes tested were then added to the wells to achieve final concentrations ranging from 10^{-6} to 10^{-4} M. Control wells were prepared by addition of culture medium (100 µL). The plates were incubated at 37°C in a 5 % CO_2 incubator for 24 h. Upon completion of the incubation, stock MTT dye solution (20 µL, 5 mg mL^{-1}) was added to each well. After 4 h, buffer (100 µL) containing *N*,*N*-dimethylformamide (50 %) and sodium dodecyl sulfate (20 %) was added to solubilize the MTT formazan. The optical density of each well was then measured with a microplate spectrophotometer at a wavelength of 490 nm. The IC_{50} values were determined by plotting the percentage viability versus concentration on a logarithmic graph and reading off the concentration at which 50 % of cells remain viable relative to the control. Each experiment was repeated at least three times to obtain the mean values. Four different tumour cell lines were the subject of this study: BEL-7402 (human hepatocellular carcinoma cell line), HeLa (human vercix adenocarcinoma cell line), MG-63 (human osteosarcoma cell line), and MCF-7 (human breast cancer cell line).

Apoptosis Studies with Acridine Orange (AO)/Ethidium Bromide (EB) Staining Method

Apoptotic studies were performed with a staining method utilising AO and EB.[17] A monolayer of BEL-7402 cells was incubated in the absence or presence of complexes **Ru-1** and **Ru-2** at concentration of 25 µM at 37°C and 5 % CO_2 for 24 h. Each cell culture was then stained with AO/EB solution (100 µg mL^{-1} AO, 100 µg mL^{-1} EB). Samples were observed under a fluorescence microscope.

Apoptosis Assay by Flow Cytometry

After chemical treatment, 1×10^6 cells were harvested, washed with phosphate-buffered saline (PBS), fixed with 70 % ethanol, and finally, maintained at 4°C for at least 12 h. The pellets were stained with a fluorescent probe solution containing 50 µg mL^{-1} propidium iodide (PI) and 1 mg mL^{-1} annexin in PBS on ice in the dark for 15 min. The fluorescence emission was then measured at 530 and 575 nm (or equivalent) using 488 nm excitation by a FACS Calibur flow cytometer

(Beckman Dickinson & Co., Franklin Lakes, NJ). A minimum of 10 000 cells were analysed.

Cellular Uptake Studies

Cells were placed in 24-well microassay culture plates (4×10^4 cells per well) and grown overnight at 37°C in a 5 % CO_2 incubator. Complexes tested were then added to the wells. The plates were incubated at 37°C in a 5 % CO_2 incubator for 48 h. Upon completion of the incubation, the wells were washed three times with PBS, after removing the culture medium in the wells. The cells were visualized by fluorescence microscopy.

Cell Cycle Arrest by Cytometric Analysis

BEL-7402 cells were seeded into six-well plates (Costar, Corning Corp, New York) at a density of 2×10^5 cells per well and incubated for 24 h. The cells were cultured in RPMI 1640 supplemented with fetal bovine serum (FBS, 10 %) and incubated at 37°C and 5 % CO_2. The medium was removed and replaced with medium (final DMSO concentration, 1 % v/v) containing complexes **Ru-1**–**4** (25 and 50 μM). After incubation for 24 h, the cell layer was trypsinized, washed with cold PBS, and fixed with 70 % ethanol. RNAse (20 mL, 0.2 mg mL^{-1}) and 20 mL of PI (0.02 mg mL^{-1}) were added to the cell suspensions and they were incubated at 37°C for 30 min. The samples were then analysed with a FACSCalibur flow cytometer (Becton Dickinson & Co., Franklin Lakes, NJ). The number of cells analysed for each sample was 10 000.[18]

Mitochondrial Membrane Potential Assay

Cells were treated for 24 h with complexes in 12-well plates and were then washed three times with cold PBS. The cells were then detached with trypsin-EDTA solution. Collected cells were incubated for 20 min with 1 μg mL^{-1} of JC-1 (5,5′,6,6′-tetrachloro-1,1′,3,3′-tetraethylbenzimidazolcarbocyanine iodide) in culture medium at 37°C in the dark. Cells were immediately centrifuged to remove the supernatant. Cell pellets were suspended in PBS and then photographed under a microscope.

DNA Binding and Photoactivated Cleavage

The DNA binding and photoactivated cleavage experiments were performed at room temperature. Buffer A (5 mM tris (hydroxymethyl)aminomethane (Tris) hydrochloride, 50 mM NaCl, pH 7.0) was used for absorption titrations, luminescence titrations, and viscosity measurements. Buffer B (50 mM Tris-HCl, 18 mM NaCl, pH 7.2) was used for DNA photocleavage experiments. The absorption titrations of the complexes in buffer were performed using a fixed concentration (20 μM) for complexes to which increments of the DNA stock solution were added. Ru–DNA solutions were allowed to incubate for 5 min before the absorption spectra were recorded.

Results and Discussion

Synthesis and Characterization

The ligand NHPIP was synthesized by condensing 1,10-phenanthroline-5,6-dione, 3-nitro-4-hydroxyphenylaldehyde, and ammonium acetate in glacial acetic acid. The ligand AHPIP was prepared by reducing NHPIP in ethanol with Pd/C and $NH_2NH_2 \cdot H_2O$. The complexes **Ru-1**–**4** were prepared in high yield by direct reaction of NHPIP or AHPIP with appropriate precursor complexes in ethylene glycol. The desired Ru^{II} complexes were isolated as the perchlorates and purified by column chromatography. In the ES-MS of the complexes, the signals of $[M - 2ClO_4 - H]^+$ and $[M - 2ClO_4]^{2+}$ were observed. The ES-MS results are given in the Experimental section. The observed molecular weights are consistent with the expected values.

Cytotoxicity Assay In Vitro

The cytotoxicity of complexes **Ru-1**–**4** towards the above cell lines was assayed by cell survival using the MTT method. Cisplatin was used as a positive control. The cell viability is depicted in Fig. 1, and the IC_{50} values are listed in Table 1. Unexpectedly, **Ru-1** shows no cytotoxicity towards BEL-7402, HeLa, and MG-63 cell lines. **Ru-2** and **Ru-4** show higher activity than **Ru-1** and **Ru-3**, respectively. Comparing the IC_{50} values, **Ru-4** shows the highest cytotoxic activity to BEL-7402 cells with the lowest IC_{50} value (13.6 ± 1.2 μM) among the four complexes. The cytotoxic potency of **Ru-4** on BEL-7402 cells is higher than that of complex $[Ru(bpy)_2(hnip)]^{2+}$ ($IC_{50} = 39.2$ μM, hnip = 2-(2-hydroxy-1-naphthyl)imidazo[4,5-*f*][1,10]phenanthroline),[19] and is similar to those of $[Ru(phen)_2(BHIP)]^{2+}$ ($IC_{50} = 20.6$ μM, BHIP = 2-(3-bromo-4-hydroxyphenyl)imizado[4,5-*f*][1,10]phenanthroline),[20] $[Ru(phen)_2(dcdppz)]^{2+}$ ($IC_{50} = 16.9$ μM, dcdppz = h,j-dichlorodipyrido[3,2-*a*:2′,3′-*c*]phenanzine),[21] and cisplatin. However, **Ru-1**, **Ru-2**, and **Ru-3** are less cytotoxic than cisplatin against the selected cell lines. In addition, Fig. 1 shows that cell viability was found to be concentration dependent, and the cell viability decreased on increasing the concentrations of complexes **Ru-1**–**4**. **Ru-4** shows the highest antitumour activity among the four complexes. The different antitumour activity of the four complexes, on the one hand, is due to the different ancillary ligands. On going from bpy to phen, the plane area and hydrophobicity increase, leading to a higher antitumour activity for **Ru-4**. On the other hand, an amino group as substituent may enhance the antitumour activity.

Apoptosis Studies by the AO/EB Staining Method

AO can pass the cell membrane of living or early apoptotic cells, while staining by EB indicates loss of membrane integrity. Under a fluorescence microscope, living cells appear green, necrotic cells stain red but have a nuclear morphology resembling that of viable cells. In the control (Fig. 2a), the living cells are stained bright green in spots. After treatment of BEL-7402 cells with 25 μM of **Ru-1** and **Ru-2** for 24 h, the green apoptotic cells with apoptotic features such as nuclear shrinkage, chromatin condensation, as well as red necrotic cells, were observed (Fig. 2b and c). Similar results were also found for complexes **Ru-3** and **Ru-4**.

Apoptosis Assay by Flow Cytometry

Induction of apoptosis is one of the considerations in drug development, most of the cytotoxic anticancer drugs in current use have been shown to induce apoptosis in susceptible cells.[22] The morphological apoptosis studies shows that these complexes can effectively induce BEL-7402 cell apoptosis. In order to determine the percentage of apoptotic and necrotic cells, the apoptotic assay was investigated by flow cytometry. After exposure of **Ru-2**, **Ru-3**, and **Ru-4** (25 μM) to BEL-7402 cells for 24 h, the percentage of living, necrotic, and apoptotic cells is shown in Fig. 3. The percentage of apoptotic cells was 25.42, 15.85, and 40.47 % for **Ru-2**, **Ru-3**, and **Ru-4**, respectively,

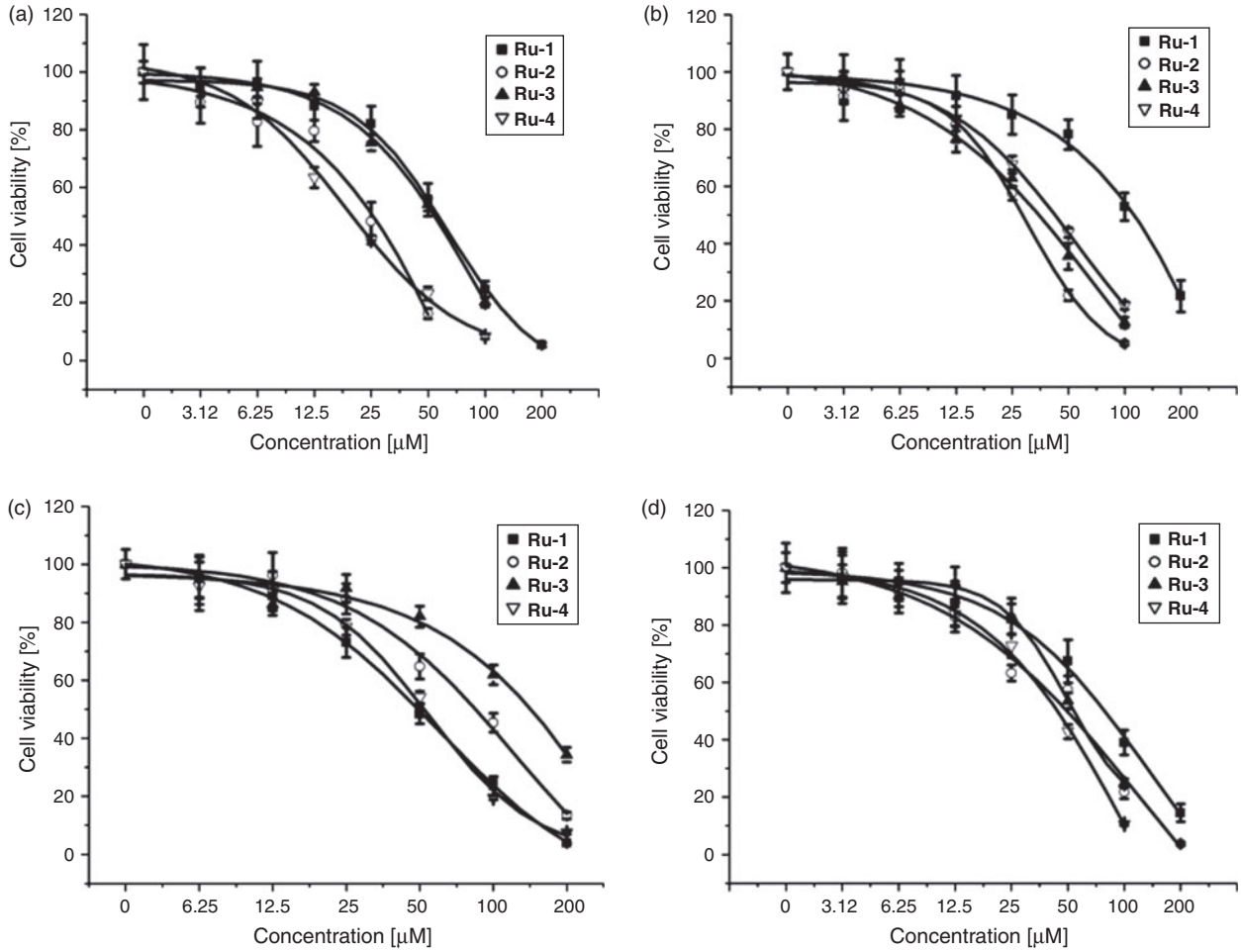

Fig. 1. Cell viability of (a) BEL-7402, (b) HeLa, (c) MCF-7, and (d) MG-63 cell proliferation in vitro induced by **Ru-1**, **Ru-2**, **Ru-3**, and **Ru-4** (see main text for definition of cell types and full complex identities). Each point is the mean ± standard error obtained from three independent experiments.

Table 1. The IC_{50} (half maximal inhibitory concentration) values of Ru-1–4 against selected cell lines

See main text for definition of cell types and full complex identities

Complexes	IC_{50} [μM]			
	BEL-7402	HeLa	MCF-7	MG-63
Ru-1	>100	>100	57.7 ± 4.7	>100
Ru-2	43.9 ± 4.4	78.7 ± 6.2	46.3 ± 3.8	67.7 ± 5.5
Ru-3	44.5 ± 4.1	82.3 ± 5.8	18.9 ± 1.6	65.6 ± 5.1
Ru-4	13.6 ± 1.2	18.6 ± 1.8	24.7 ± 2.6	34.3 ± 3.1
Cisplatin	19.4 ± 2.3	18.1 ± 1.6		6.6 ± 0.4

which is consistent with the IC_{50} values. Complex **Ru-4** showed the highest apoptotic effect among the three complexes.

Cellular Uptake Studies

In the functional study, the efficacy of **Ru-1**–**4** was evaluated on human hepatocellular carcinoma BEL-7402 cells. The uptake of these complexes by BEL-7402 cells was studied using a fluorometric method. **Ru-1**–**4** (25 μM) was added to the wells (4×10^4 cells per well) and incubated at 37°C in a 5% CO_2 incubator for 24 h. The wells were then washed three times with PBS, and after discarding the culture medium, the cells were observed under a fluorescent microscope. As shown in Fig. 4, after treatment of BEL-7402 cells with the four complexes, bright red fluorescent spots in the images were observed. The results show that these complexes can be uptaken by cells, and they can enter into the cytoplasm and accumulate in the nuclei. Similar results were observed for other ruthenium(II) polypyridyl complexes.[23,24]

*Effect of **Ru-1–4** on the Cell Cycle Distribution*

BEL-7402 cells were treated with 25 or 50 μM of **Ru-1**–**4** for 24 h, and the distribution of cells in various compartments during the cell cycle was analysed by flow cytometry in PI-stained cells. The cell cycle distribution is shown in Fig. 5. When the concentration of these complexes reached 50 μM, an obvious enhancement (10.48, 7.76, 5.15, and 7.04% for **Ru-1**, **Ru-2**, **Ru-3**, and **Ru-4**) in the percentage of cells at the G0/G1 phase was observed, accompanied by a corresponding reduction (10.39, 2.62, 4.51, and 2.99% for **Ru-1**, **Ru-2**, **Ru-3**, and **Ru-4**) in the percentage of cells in the S phase (Fig. 5b). In addition, at a concentration of 25 μM, these complexes also induced an increase at the G0/G1 phase (Fig. 5a). These results suggest the antiproliferative mechanism induced by the complexes on BEL-7402 cells is G0/G1 phase arrest.

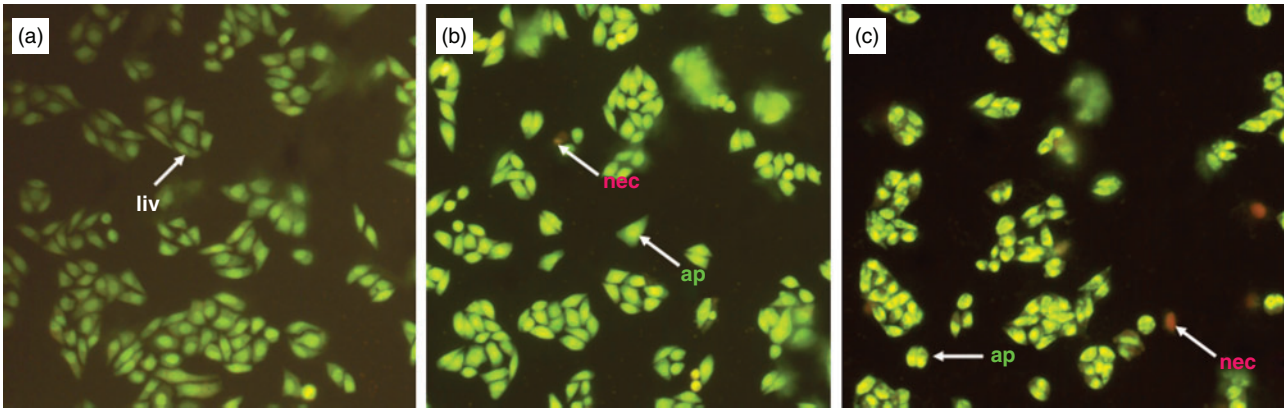

Fig. 2. BEL-7402 (human hepatocellular carcinoma cell line) cells were stained by acridine orange (AO)/ethidium bromide (EB) and observed under fluorescence microscopy. (a) Control, (b) exposure to 25 μM of **Ru-1**, and (c) exposure to **Ru-2** incubated at 37°C and 5 % CO_2 for 24 h. Liv: living cells, ap: apoptotic cells; nec: necrotic cells.

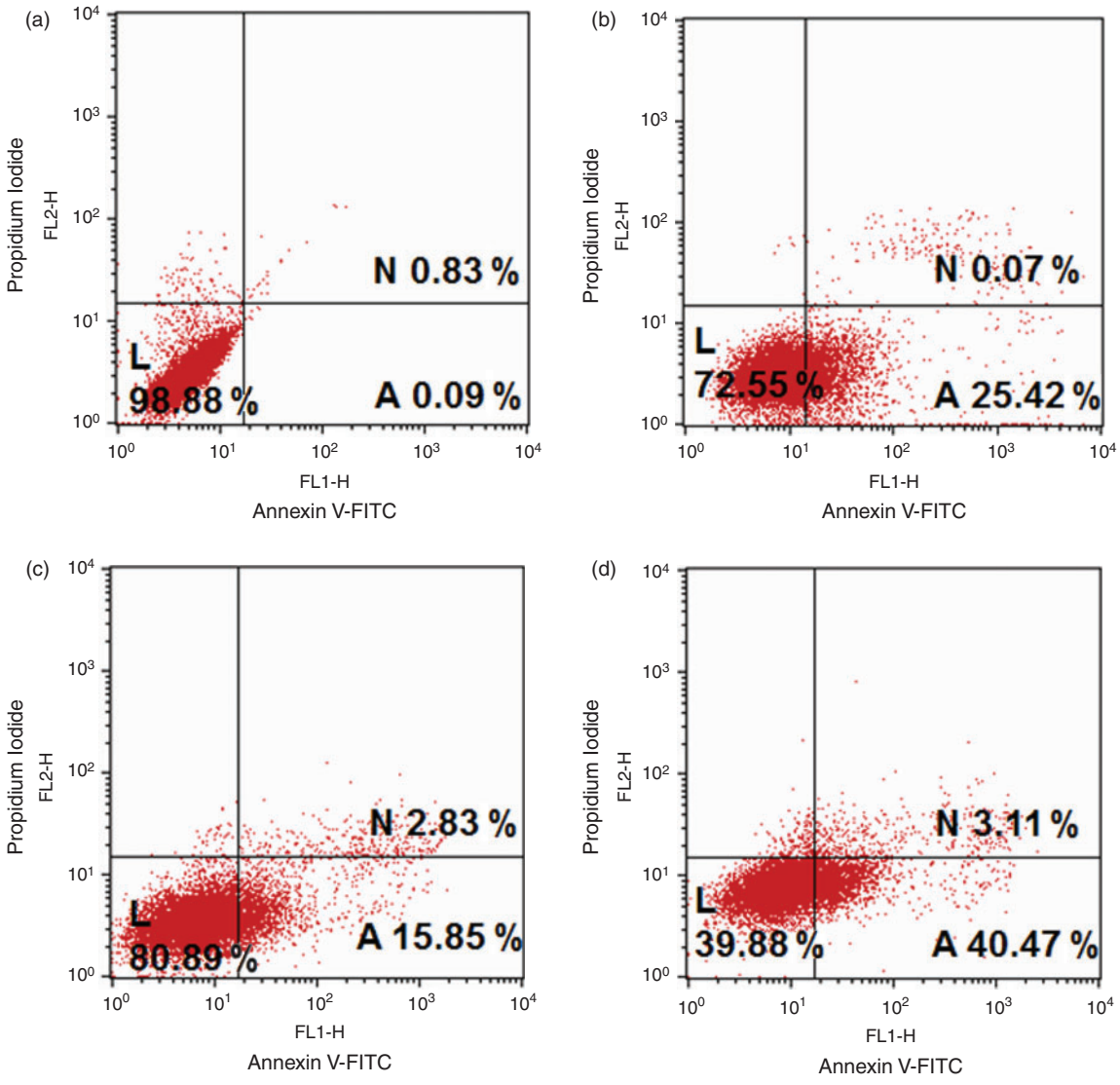

Fig. 3. The percentage of living (L), necrotic (N), and apoptotic (A) ruthenium complex-treated BEL-7402 (human hepatocellular carcinoma cell line) cells as analysed by FACS calibur flow cytometry. (a) Control. After 24 h exposure to 25 μM of (b) **Ru-2**, (c) **Ru-3**, and (d) **Ru-4**. (See main text for full complex identities.)

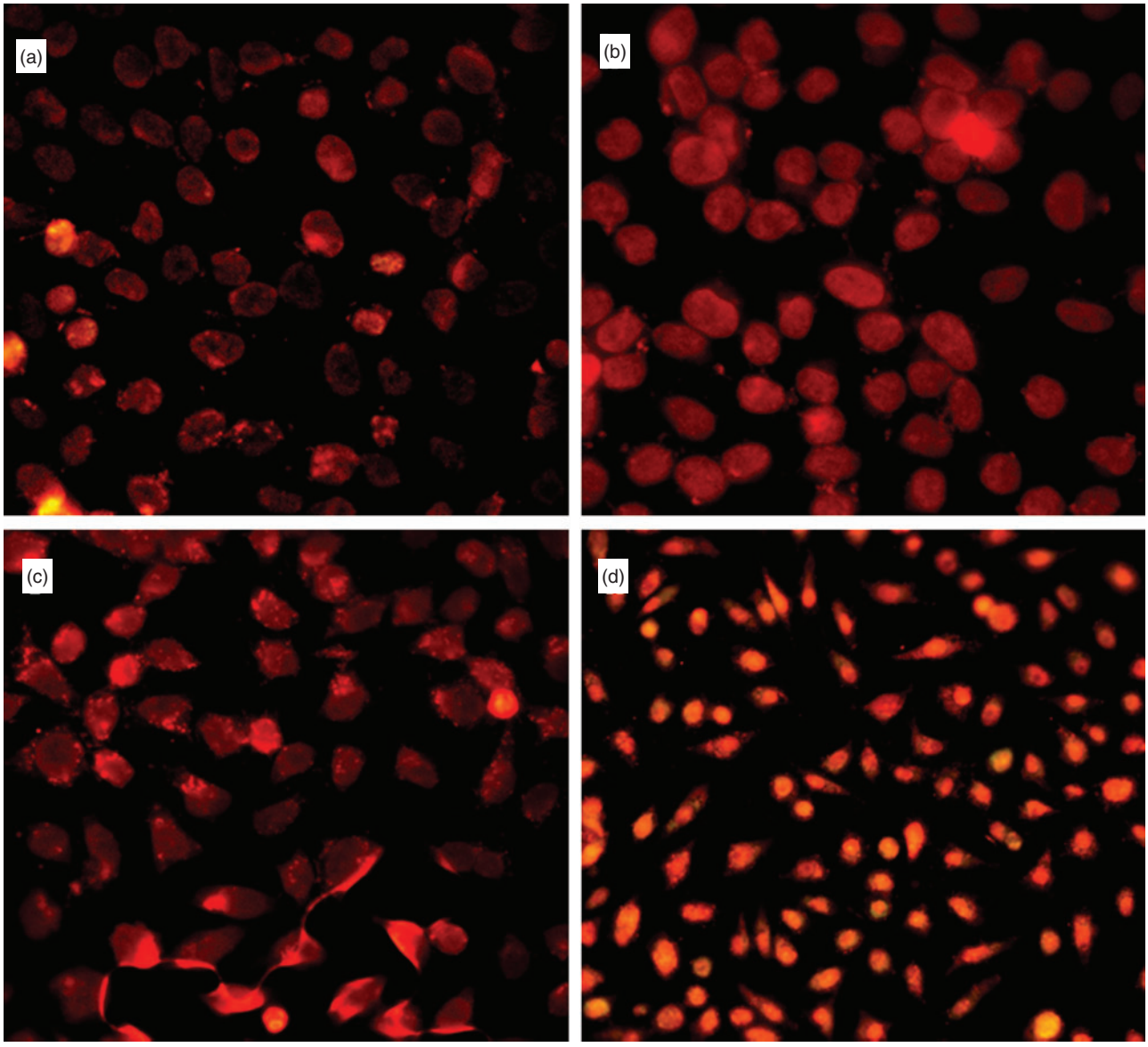

Fig. 4. BEL-7402 (human hepatocellular carcinoma cell line) cells incubated with 25 μM of (a) **Ru-1**, (b) **Ru-2**, (c) **Ru-3**, and (d) **Ru-4** for 24 h, imaged by fluorescence microscopy. (See main text for full complex identities.)

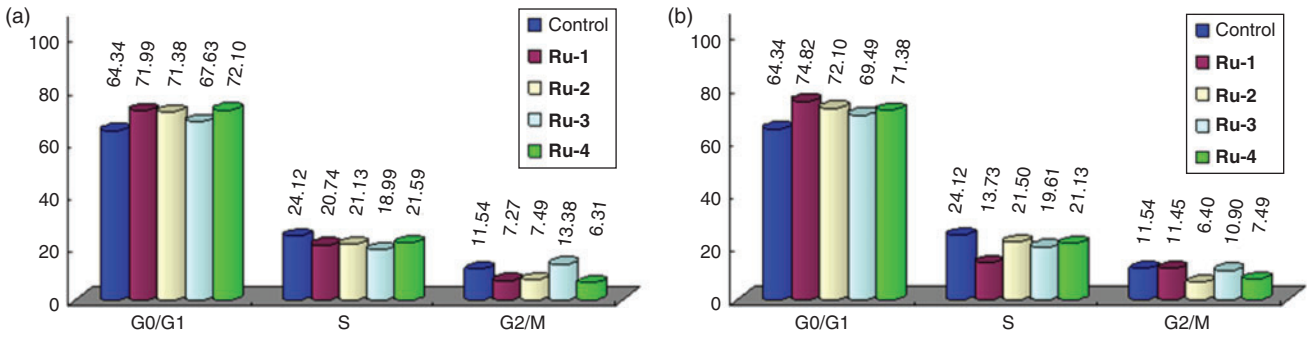

Fig. 5. Cell cycle distribution of BEL-7402 (human hepatocellular carcinoma cell line) cells with (a) 25 and (b) 50 μM of complexes **Ru-1**–**4** incubated for 24 h. (See main text for full complex identities and description of cell cycle phases.)

Mitochondrial Membrane Potential Detection

JC-1 was used as a fluorescence probe in detecting the change of mitochondrial membrane potential induced by complexes **Ru-1** and **Ru-2**. At high mitochondrial membrane potential, JC-1 forms aggregates, which have a red fluorescence emission peak. At low mitochondrial membrane potential, JC-1 forms monomers, which emit a green fluorescence peak. As shown in Fig. 6, in the control, JC-1 exhibits a red fluorescence (JC-1 aggregates)

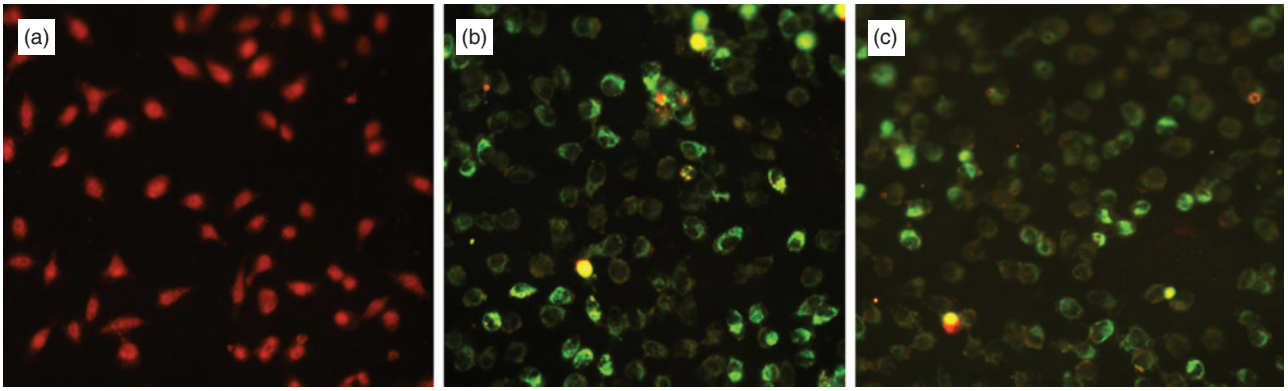

Fig. 6. Assay of BEL-7402 (human hepatocellular carcinoma cell line) cells' mitochondrial membrane potential with JC-1 (5,5′,6,6′-tetrachloro-1,1′,3,3′-tetraethylbenzimidazolcarbocyanine iodide) as fluorescence probe. (a) Control. After 24 h exposure to 12.5 μM of (b) **Ru-1** and (c) **Ru-2**. (See main text for full complex identities.)

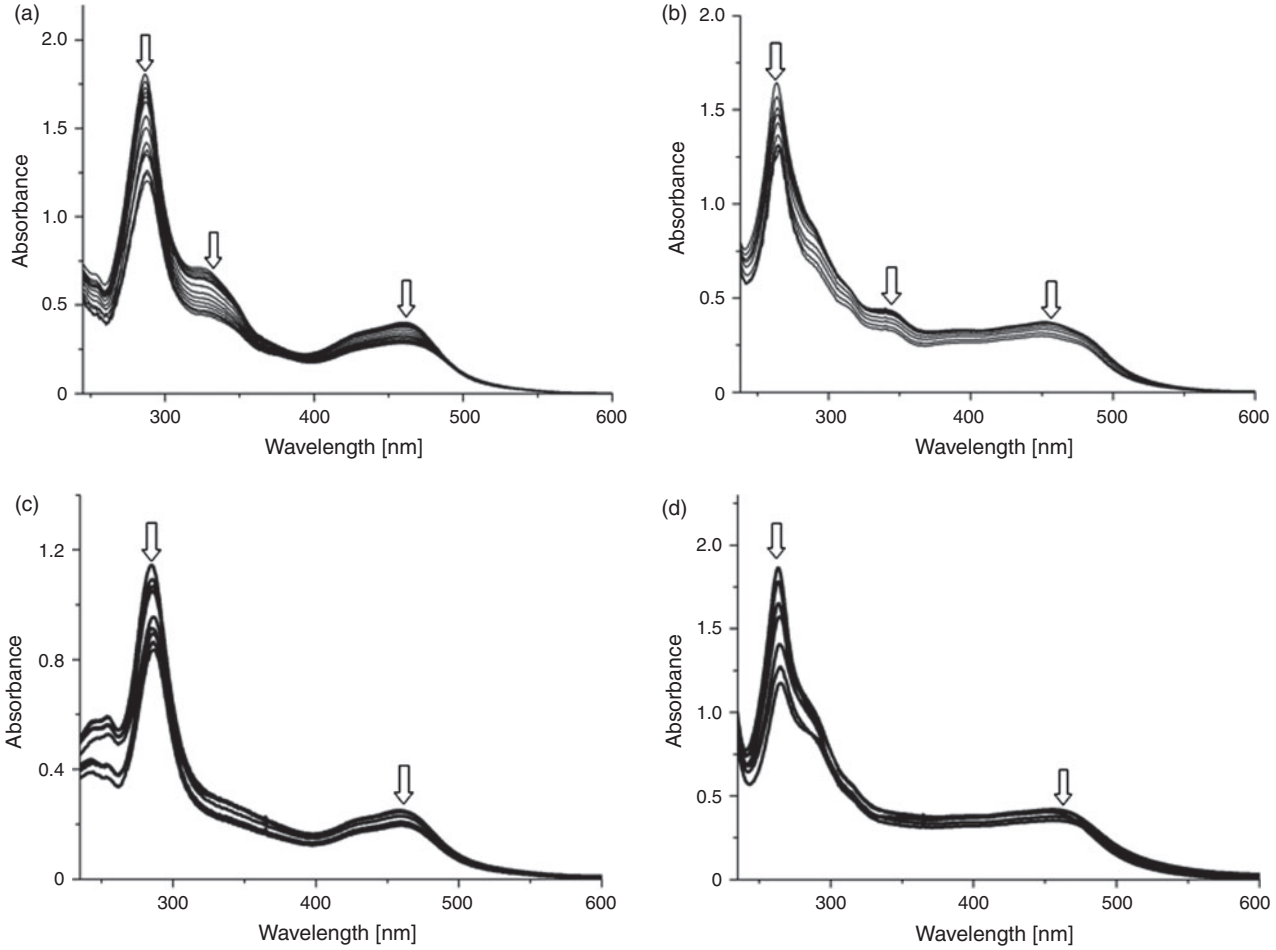

Fig. 7. Absorption spectra of complexes in Tris-HCl buffer upon addition of calf thymus-DNA in the presence of complexes (a) **Ru-1**, (b) **Ru-2**, (c) **Ru-3**, and (d) **Ru-4**. [Ru] = 20 μM. Arrow shows the absorbance change upon the increase of DNA concentration. (See main text for full complex identities.)

with high mitochondrial membrane potential. After BEL-7402 cells are exposed to 12.5 μM **Ru-1** and **Ru-2** for 24 h, JC-1 shows a green fluorescence (JC-1 monomers) corresponding to low mitochondrial membrane potential. The change from red to green fluorescence suggests the decrease of mitochondrial membrane potential in the presence of **Ru-1** and **Ru-2**. These results indicated that **Ru-1** and **Ru-2** induced apoptosis in BEL-7402 cells through the mitochondrial signal transduction pathway.

Electronic Absorption Spectra Studies

The absorption spectra of complexes **Ru-1**–**4** mainly consist of two or three resolved bands in the range 200–600 nm. The lowest energy bands at 460 nm for **Ru-1**, 453 nm for **Ru-2**,

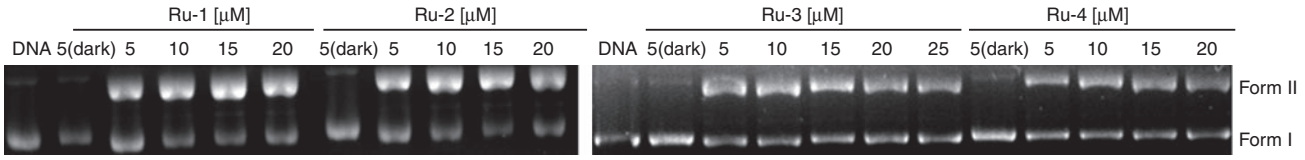

Fig. 8. Photoactivated cleavage of pBR322 DNA in the presence of different concentrations of complexes upon irradiation at 365 nm for 30 min. (See main text for full complex identities and form of DNA.)

459 nm for **Ru-3**, and 451 nm for **Ru-4** are assigned to the metal-to-ligand charge transfer (MLCT) transition. The bands in the range of 300–400 nm are attributed to π–π* transitions. The bands below 300 nm are attributed to intraligand (IL) π–π* transitions. Fig. 7 shows the absorption spectra of complexes **Ru-1** to **Ru-4** in the presence of increasing concentration of DNA. As the concentration of calf thymus DNA (CT-DNA) increases, the MLCT transition band of complexes **Ru-1**–**4** exhibit hypochromism of 29.85, 29.84, 24.70, and 21.92 %, respectively. Due to the intercalative mode involving a stacking interaction between the aromatic chromophore and the DNA base pairs, a large change in absorbance can be observed while a complex binds to DNA through intercalative mode of binding.

DNA Photocleavage

When circular plasmid DNA is subject to electrophoresis, relatively fast migration will be observed for the intact supercoiled form (Form I). If scission occurs on one strand (nicked), the supercoiled form will relax to generate a slower-moving open circular form (Form II).[25] The cleavage of plasmid DNA in the absence or presence of complexes **Ru-1**–**4** was monitored by agarose gel electrophoresis. The DNA cleaving efficiencies of these complexes are shown in Fig. 8. No obvious DNA cleavage was observed for controls in which the complex was absent, or for incubation of the plasmid with the Ru^{II} complex in the dark. In the presence of different concentrations of the complexes, the amount of Form I of pBR322 DNA diminishes, whereas that of Form II increases. These results indicated that these complexes can effectively cleave pBR322 DNA upon irradiation.

Conclusions

Four new ruthenium(II) polypyridyl complexes **Ru-1**–**4** were synthesized and characterized. AO/EB staining methods showed that these complexes can effectively induce apoptosis of BEL-7402 cells. Apoptotic assay by flow cytometry exhibited that the number of apoptotic cells increased with increasing concentration of complexes. The cellular uptake studies showed that the complexes can be successfully uptaken and complexes entered into the cytoplasm. The cell cycle distribution demonstrated that the antiproliferative mechanism induced by the four complexes on BEL-7402 cells was G0/G1 phase arrest. In addition, **Ru-1** and **Ru-2** induced a decrease of the mitochondrial membrane potential. These results indicated that the complexes induced apoptosis of BEL-7402 cells through the mitochondrial signal transduction pathway. Upon irradiation, these ruthenium(II) complexes can effectively cleave pBR 322 DNA.

Disclosure Statement

No competing financial interest exists.

Acknowledgements

This work was supported by the National Nature Science Foundation of China (No 31070858) and Guangdong Pharmaceutical University for financial support.

References

[1] K. E. Erkkila, D. T. Odom, J. K. Barton, *Chem. Rev.* **1999**, *99*, 2777. doi:10.1021/CR9804341
[2] P. Bhattacharya, J. K. Barton, *J. Am. Chem. Soc.* **2001**, *123*, 8649. doi:10.1021/JA010996T
[3] S. Delaney, J. Yoo, E. D. A. Stemp, J. K. Barton, *Proc. Natl. Acad. Sci. USA* **2004**, *101*, 10511. doi:10.1073/PNAS.0403791101
[4] B. H. Yun, J. O. Kim, B. N. Lee, P. Lincoln, N. Norden, J. M. Kim, S. K. Kim, *J. Phys. Chem. B* **2003**, *107*, 9858. doi:10.1021/JP027828N
[5] L. F. Tan, J. Liu, J. L. Shen, X. H. Liu, L. L. Zeng, L. H. Jin, *Inorg. Chem.* **2012**, *51*, 4417. doi:10.1021/IC300093H
[6] U. Schatzschneider, J. Niesel, I. Ott, R. Gust, H. Alborzinia, S. Wölfl, *ChemMedChem* **2008**, *3*, 1104. doi:10.1002/CMDC.200800039
[7] D. D. Sun, Y. N. Liu, D. Liu, R. Zhang, X. C. Yang, J. Liu, *Chem.–Eur. J.* **2012**, *18*, 4285. doi:10.1002/CHEM.201103156
[8] B. S. Howerton, D. K. Heidary, E. C. Glazer, *J. Am. Chem. Soc.* **2012**, *134*, 8324. doi:10.1021/JA3009677
[9] V. Rajendiran, M. Murali, E. Suresh, M. Palaniandavar, V. S. Periasamy, M. A. Akbarsha, *Dalton Trans.* **2008**, *38*, 2157. doi:10.1039/B715077F
[10] Y. J. Liu, C. H. Zeng, Z. H. Liang, J. H. Yao, H. L. Huang, Z. Z. Li, F. H. Wu, *Eur. J. Med. Chem.* **2010**, *45*, 3087. doi:10.1016/J.EJMECH.2010.03.042
[11] H. L. Huang, Z. Z. Li, Z. H. Liang, J. H. Yao, Y. J. Liu, *Eur. J. Med. Chem.* **2011**, *46*, 3282. doi:10.1016/J.EJMECH.2011.04.049
[12] Y. J. Liu, Z. H. Liang, Z. Z. Li, J. H. Yao, H. L. Huang, *J. Organomet. Chem.* **2011**, *696*, 2728. doi:10.1016/J.JORGANCHEM.2011.04.020
[13] Y. J. Liu, Z. Z. Li, Z. H. Liang, J. H. Yao, H. L. Huang, *DNA Cell Biol.* **2011**, *30*, 839. doi:10.1089/DNA.2011.1243
[14] W. Paw, R. Eisenberg, *Inorg. Chem.* **1997**, *36*, 2287. doi:10.1021/IC9610851
[15] B. P. Sullivan, D. J. Salmon, T. J. Meyer, *Inorg. Chem.* **1978**, *17*, 3334. doi:10.1021/IC50190A006
[16] T. Mosmann, *J. Immunol. Methods* **1983**, *65*, 55. doi:10.1016/0022-1759(83)90303-4
[17] *Cells: A Laboratory Manual* (Eds D. L. Spector, R. D. Goldman, L. A. Leinwand) **1998**, Vol. 1, Ch. 15 (Cold Spring Harbour Laboratory Press: New York, NY).
[18] K. K. Lo, T. K. Lee, J. S. Lau, W. L. Poon, S. H. Cheng, *Inorg. Chem.* **2008**, *47*, 200. doi:10.1021/IC701735Q
[19] L. F. Tan, F. C. Song, X. Q. Zou, X. L. Ling, *DNA Cell Biol.* **2011**, *30*, 277. doi:10.1089/DNA.2010.1137
[20] Q. F. Guo, S. H. Liu, Q. H. Liu, H. H. Xu, J. H. Zhao, H. F. Wu, X. Y. Li, J. W. Wang, *DNA Cell Biol.* **2012**, *31*, 1205. doi:10.1089/DNA.2011.1490
[21] J. A. Hickman, *Cancer Metastasis Rev.* **1992**, *11*, 121. doi:10.1007/BF00048059
[22] H. L. Huang, Z. Z. Li, Z. H. Liang, Y. J. Liu, *Eur. J. Inorg. Chem.* **2011**, *36*, 5538. doi:10.1002/EJIC.201100848
[23] C. T. Poon, P. S. Chan, C. Man, F. L. Jiang, R. N. S. Wong, N. K. Mak, D. W. J. Kwong, S. W. Tsao, W. K. Wong, *J. Inorg. Biochem.* **2010**, *104*, 62. doi:10.1016/J.JINORGBIO.2009.10.004
[24] O. Zava, S. M. Zakeeruddin, C. Danelon, H. Vogel, M. Grätzel, P. J. Dyson, *ChemBioChem* **2009**, *10*, 1796. doi:10.1002/CBIC.200900013
[25] J. K. Barton, A. L. Raphael, *J. Am. Chem. Soc.* **1984**, *106*, 2466. doi:10.1021/JA00320A058